ARTICLES
https://doi.org/10.1038/s41558-021-01108-4

nature climate change

Check for updates

Differences in the temperature dependence of wetland CO_2 and CH_4 emissions vary with water table depth

Hongyang Chen, Xiao Xu, Changming Fang, Bo Li and Ming Nie ✉

Wetland CH_4 emissions have been demonstrated to be more sensitive than wetland CO_2 emissions to increasing temperatures, which may result in a greater relative contribution of CH_4 to total GHG emissions under climate warming. However, it is not clear whether this greater sensitivity occurs globally across diverse hydrologic regimes. Here, we evaluate the temperature dependence of CO_2 and CH_4 emissions on water table depth using a global database and show similarities in the temperature dependence of CO_2 and CH_4 emissions. A lower water table is associated with a decrease in the temperature dependence of CH_4 emissions and a higher water table has the opposite effect. Water table depth does not affect the temperature dependence of CO_2 emissions. Our findings suggest the stimulatory effect of increasing temperature on wetland CH_4 emissions may not always be stronger than that on CO_2 emissions and depends on the wetland water table.

Wetlands cover only ~8% of the total land area on Earth[1] but store 29–45% of the terrestrial organic carbon (C) (refs. [2–4]). Carbon dioxide (CO_2) and methane (CH_4) are the dominant gaseous end-products of the remineralization of organic C as well as the two greatest contributors to the anthropogenic greenhouse effect[5,6]. Increasing temperature is expected to accelerate the decomposition of wetland organic C, stimulating additional soil CO_2 and CH_4 emissions and triggering a positive soil C–climate feedback loop[7–9]; this effect is especially notable for CH_4, a particularly potent GHG that has 34 times the radiative forcing potential of CO_2 by mass over the course of a century[6,10]. Temperature dependence represents a key parameter of previously developed biogeochemical models that simulate GHG emissions[8,11,12]. When these models are applied at regional and global scales, small inaccuracies in this parameter can result in large errors[8,10,11,13]. Quantifying the temperature dependence of the emissions of these GHGs is thus critical to projections of the feedbacks among wetland ecosystems, C cycling and climate change[8,14].

However, there is substantial uncertainty regarding the temperature dependence of wetland GHG emissions[7,10,15,16]. The activation energy is the lowest amount of energy required to initiate a reaction[11] and temperature dependence can be described in terms of the apparent activation energy which describes the emergent response of many biotic and abiotic processes associated with GHG effluxes[17,18]. Studies of the temperature dependence of ecosystem-level CH_4 emissions have reported highly variable apparent activation energies of 0.2–2.5 eV ($1\,eV = 96\,kJ\,mol^{-1}$)[7,18–21]. Numerous experiments under both field and short-term laboratory conditions have shown that CH_4 efflux is more sensitive to temperature change than CO_2 efflux due to the differences in the biochemical kinetics of methanogenesis and respiration[10,19,22–24]. Consistent with this conclusion, a global meta-analysis by Yvon-Durocher et al.[18] showed that the temperature dependence of CH_4 efflux (corresponding to an activation energy of 0.96 eV) was considerably higher than that of CO_2 efflux (0.65 eV), resulting in a higher CH_4:CO_2 emission ratio as the temperature increased. This increase in the CH_4:CO_2 emission ratio suggests that wetland ecosystems around the world may become more methanogenic in the future[5,25], leading to stronger positive feedbacks between global warming and C cycling.

It remains unclear whether CH_4 emissions are invariably more sensitive to temperature change than CO_2 emissions. The majority of the most relevant previous studies were performed in wetland ecosystems with water-saturated soils or under anaerobic soil incubation conditions[10,18,19,22–24] but wetland topsoil is not always water-saturated and is often subject to water table fluctuations[26–28]. Previous studies have shown that the threshold water table depth (WTD) of global wetlands ranges from −150 to 0 cm (refs. [29,30]) and even a small change in the wetland WTD may have profound impacts on the relative importance of GHGs in terms of overall C emissions[27,31–33]. Until now, however, there has been a lack of global-scale evaluation of the temperature dependence of CO_2 and CH_4 emissions from diverse wetland ecosystems representing diverse climatic and hydrological regimes.

Here, we compiled a database comprising 3,345 paired observations of seasonally measured CO_2 and CH_4 emissions from 204 field sites around the world that encompasses a very wide range of wetland ecosystem types and hydrological regimes (Extended Data Fig. 1). We then used these data to assess the temperature dependence of wetland CO_2 and CH_4 emissions and analysed different WTD intervals to determine whether these relationships changed with variations in WTD.

The analysis of the field data revealed exponential relationships between wetland GHG emissions and temperature across 204 sites (Extended Data Fig. 2). To characterize the temperature dependence of wetland CO_2 and CH_4 emissions, we fitted the Boltzmann–Arrhenius function[17,18,34] (which describes the exponential relationship between metabolic rates and temperature) to the data in our global database and then evaluated this temperature dependence using a linear mixed-effects model. The analysis of wetland CO_2 and CH_4 emission rates revealed that the estimated average apparent

Ministry of Education Key Laboratory for Biodiversity Science and Ecological Engineering, National Observations and Research Station for Wetland Ecosystems of the Yangtze Estuary, Institute of Biodiversity Science and Institute of Eco-Chongming, School of Life Sciences, Fudan University, Shanghai, China. ✉e-mail: mnie@fudan.edu.cn

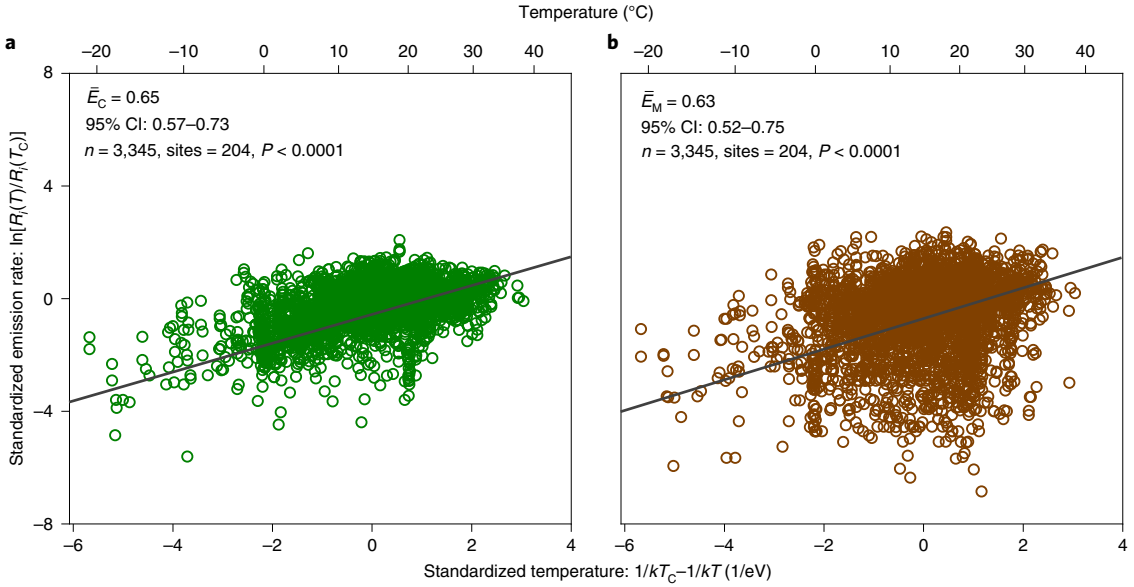

Fig. 1 | Temperature dependence of wetland CO_2 and CH_4 emissions. a,**b**, The temperature dependence values of wetland CO_2 (**a**) and CH_4 (**b**) emissions were separately characterized using mixed-effects models after fitting Boltzmann–Arrhenius functions to the emissions data with site-level random effects on the apparent activation energy and emission rate at a fixed temperature (Methods). The fitted solid lines correspond to the average apparent activation energies estimated from the mixed-effects models ($\overline{E_C}$ = 0.65 eV for the CO_2 emissions (**a**) and $\overline{E_M}$ = 0.63 eV for the CH_4 emissions (**b**)). Emissions are expressed in standardized form as ln[$R_i(T)/R_i(T_C)$], where $R_i(T)$ is the measured CO_2 or CH_4 emission rate at site i and $R_i(T_C)$ is the site-specific estimate of the CO_2 or CH_4 emission rate at a fixed temperature (T_C = 14.7 °C, the average measured temperature in the field emissions dataset). These standardizations are provided only as a visual representation of the data.

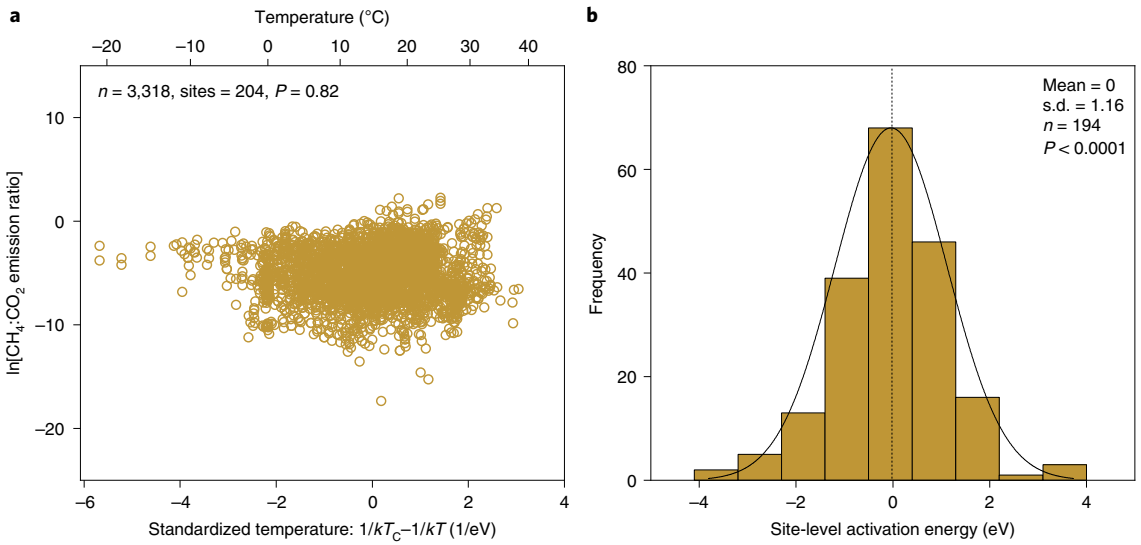

Fig. 2 | Temperature dependence of the CH_4:CO_2 emission ratio. a, The relationship between the CH_4:CO_2 emission ratio and the standardized inverse absolute temperature shown was analysed using a mixed-effects model after fitting a Boltzmann–Arrhenius function with site-level random effects on the temperature dependence and the emission ratio at a fixed temperature. **b**, The curve represents a Gaussian distribution fitted to the frequency data for the temperature dependence of the CH_4:CO_2 emission ratio. The distribution of site-level temperature dependence values yielded an average of 0 eV (represented by a dashed line in **b**). Note that 27 outliers of CH_4:CO_2 ratios were identified, and hence excluded in the analysis in **a**.

activation energy (reflecting the temperature dependence) of CO_2 emissions ($\overline{E_C}$) did not differ significantly ($P > 0.05$) from that of CH_4 emissions ($\overline{E_M}$) (Fig. 1), suggesting that CO_2 and CH_4 emissions showed similar temperature dependence. Similarly, the intersite response of CO_2 emissions to the mean temperatures at the sites was consistent with that of CH_4 emissions (Extended Data Fig. 3).

As expected from the similar responses of CO_2 and CH_4 emissions to temperature, the CH_4:CO_2 emission ratio was not significantly affected by temperature across all sites (P = 0.82; Fig. 2a). Additionally, the frequency distribution of the site-level temperature dependence of the CH_4:CO_2 emission ratio could be characterized by a Gaussian (normal) distribution, yielding an average temperature dependence of 0 eV on a global scale ($P < 0.0001$; Fig. 2b).

Our findings of the similar temperature dependence of CO_2 and CH_4 emissions and an invariant CH_4:CO_2 emission ratio with increasing ambient temperature differ from the prevailing

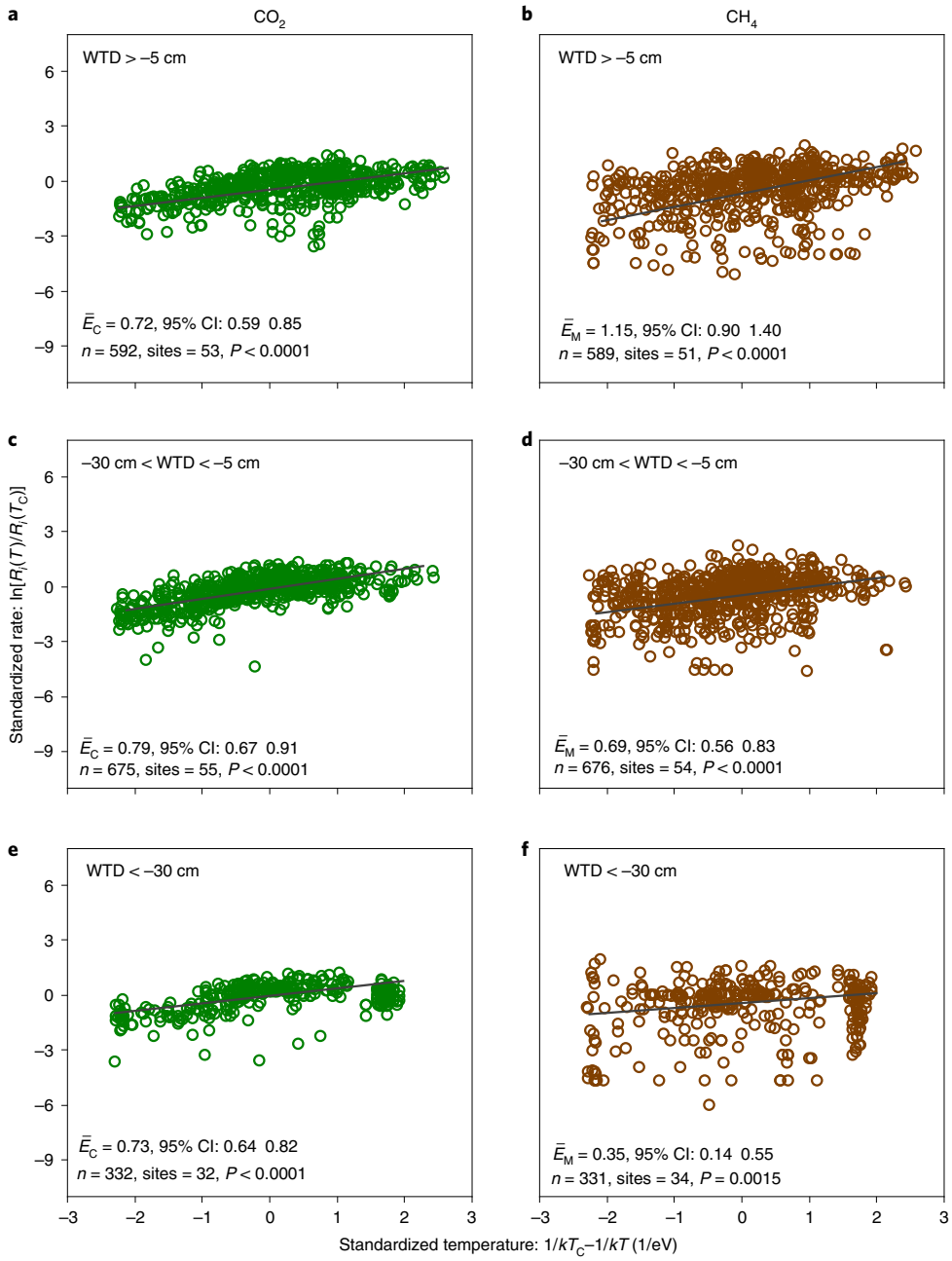

Fig. 3 | Temperature dependence of CO_2 and CH_4 emissions at different WTD ranges. a–f, The temperature dependence values of CO_2 and CH_4 emissions were separately characterized using mixed-effects models after fitting Boltzmann–Arrhenius functions to the emissions data with site-level random effects on the apparent activation energy and rate at a fixed temperature (Methods). The fitted solid lines correspond to the average apparent activation energies estimated from the mixed-effects models ($\bar{E}_C$ for CO_2 emissions (**a**,**c**,**e**) and $\bar{E}_M$ for CH_4 emissions (**b**,**d**,**f**)). WTD > -5 cm (**a**,**b**), -30 cm < WTD < -5 cm (**c**,**d**), WTD < -30 cm (**e**,**f**). Standardized emissions are expressed as $\ln[R_i(T)/R_i(T_C)]$, where $R_i(T)$ is the measured rate of CO_2 or CH_4 emissions at site *i* and $R_i(Tc)$ is the site-specific estimate of the CO_2/CH_4 emission rate at a fixed temperature (T_C = 14.7 °C, the average measured temperature in the field emissions dataset). These standardizations are provided only as a visual representation of the data.

consensus, which suggests CH_4 emissions are more sensitive to temperature than are CO_2 emissions. The majority of relevant previous laboratory and field studies were performed under water-saturated anaerobic soil conditions[10,18,19,22–24]. By contrast, the GHG emission data in our database were derived from diverse hydrological conditions spanning a wide range of WTDs. We suggest that the temperature dependence of wetland GHG emissions is likely to be altered by variations in water table in our database.

To assess the effect of WTD on the temperature dependence of GHG emissions, we further analysed a subset of the data in which WTD and CO_2 and CH_4 emissions were measured simultaneously. This dataset comprised 1,580 paired observations from 88 field sites at which the WTD was not significantly correlated with the ambient temperature (Supplementary Fig. 1). The aeration status of wetland topsoil often has a strong influence on GHG fluxes, especially CH_4 emissions[19]. Generally, when the WTD is below −30 cm, wetland topsoil is relatively well-aerated and is conducive to microbial aerobic CH_4 oxidation and CO_2 respiration[35–39]; by contrast, when the water table is close to or above the soil surface (generally WTD > −5 cm), wetland soils as a whole experience water-saturated

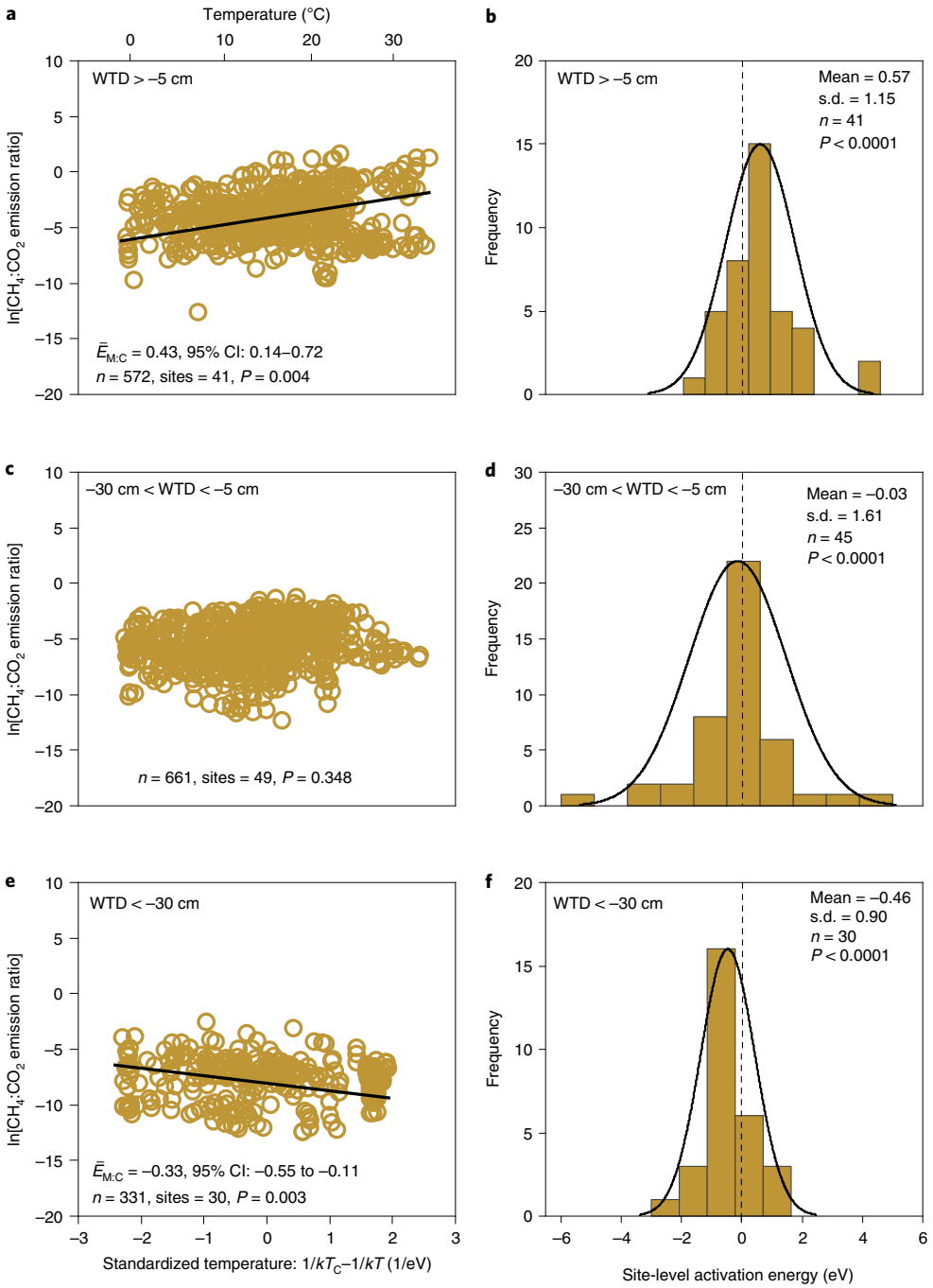

Fig. 4 | Temperature dependence of the CH_4:CO_2 emission ratio at different WTD ranges. a,**c**,**e**, The temperature dependences were separately characterized using mixed-effects models after fitting Boltzmann–Arrhenius functions to the CH_4:CO_2 emission ratio data with site-level random effects on the apparent activation energy and ratio at a fixed temperature (Methods). The fitted solid lines correspond to the average apparent activation energies ($\overline{E_{M:C}}$ for the CH_4:CO_2 emission ratio (**a**,**e**)) estimated from the mixed-effects models. **b**,**d**,**f**, The curves represent Gaussian distributions fitted to the frequency data for the temperature dependence of the CH_4:CO_2 emission ratio at different WTD ranges: WTD > –5 cm (**a**,**b**), –30 cm < WTD < –5 cm (**c**,**d**), WTD < –30 cm (**e**,**f**). The vertical dashed line represents the activation energy value = 0.

anaerobic conditions, which promote the production and release of CH_4 but suppress microbial CO_2 respiration[19,40,41]. Thus, we divided all the GHG emission data on the basis of three WTD intervals: <−30 cm, −30 to −5 cm and >−5 cm. Furthermore, by analysing the influences of temperature and water table on GHG emissions, we found that the variations in WTD significantly ($P < 0.001$) affected CO_2 and CH_4 emissions when all depths were combined but had no significant influence on CO_2 and CH_4 emissions within each of the established WTD intervals (Supplementary Table 1). These results suggest that the three WTD intervals reflected different hydrological regimes for GHG emissions.

Across the different WTD intervals, our results revealed similarities in the temperature dependence of CO_2 emissions but dissimilarities in that of CH_4 emissions (Fig. 3). Specifically, the $\overline{E_C}$ values corresponding to the different WTD intervals were statistically indistinguishable from one another, while the $\overline{E_M}$ values markedly

decreased with decreasing WTD ($P < 0.01$) (Extended Data Fig. 4). A similar pattern was also observed for the temperature dependence of CO_2 and CH_4 emissions from the sites in our database at which the water table was relatively static throughout the time period of GHG emissions measurements (Extended Data Fig. 5). The remarkable variation in the temperature dependence of CH_4 emissions with changing WTD that we observed here might partially explain the wide range in previous estimates of the temperature dependence of ecosystem-level CH_4 emissions, between 0.2 and 2.5 eV (refs. [7,18–21]). These results also support the idea that models describing CH_4 emissions based on fixed temperature dependence are inadequate to predict GHG emissions across wetland ecosystems[11] but suggest that the varying temperature dependence of CH_4 emissions can be attributed to changing WTDs.

In addition, we found that at a high water level (WTD > −5 cm), the $\overline{E_M}$ value (1.15 eV) was considerably higher ($P < 0.01$) than the $\overline{E_C}$ value (0.72 eV) (Fig. 3a,b and Extended Data Fig. 4), resulting in a significant increase in the CH_4:CO_2 emission ratio with increasing temperature (Fig. 4a,b). In contrast, when the water table was low (<−30 cm), the temperature dependence of CH_4 emissions (0.35 eV) was much weaker than that of CO_2 emissions (0.73 eV) (Fig. 3e,f and Extended Data Fig. 4), leading to a significant decline in the CH_4:CO_2 emission ratio as the temperature increased (Fig. 4e,f). These contrasting results indicate that with increasing ambient temperature, the relative contribution of CH_4 to overall GHG emissions might be enhanced in ecosystems with permanently water-saturated soils but reduced in those with lower water tables.

However, at intermediate WTD levels (from −30 to −5 cm), CO_2 and CH_4 emissions showed similar temperature dependence (Fig. 3c,d and Extended Data Fig. 4) and the CH_4:CO_2 emission ratio did not significantly change with increasing temperature (Fig. 4c,d). The site-level mean WTDs in this dataset followed a Gaussian distribution ($P < 0.0001$), with an average of −18 cm ranging from −144 to 134 cm (Extended Data Fig. 6); this dataset reflects the water-level characteristics of global wetlands[29,30]. Most mean WTD values at the sites considered in our study were between −30 and −5 cm (Extended Data Fig. 6) and the global average wetland WTD (−25 cm) also falls within this range[29,30]. Thus, the dominance of the intermediate WTD category may help explain the observed consistency in the temperature dependence of CO_2 and CH_4 emissions on a global scale (Fig. 1 and Supplementary Fig. 2).

Wetlands represent transitional zones between aquatic and terrestrial environments. Their hydrology is projected to be affected by global climate change and these effects are expected to show substantial spatial variation[42]. Specifically, wetlands in some places (for example, the Mediterranean) will become drier, while those in others (for example, Northern Hemisphere high latitudes) will become wetter; the general projected global trend is towards drying[6,43]. In addition to the weaker temperature dependence of CH_4 compared to that of CO_2 emissions at lower water levels (Fig. 3e,f), our analysis of field data further showed that the lower water tables (<−30 cm) could significantly increase CO_2 emissions but decrease CH_4 emissions and that the higher water tables (>−5 cm) have the opposite effect (Supplementary Fig. 3). A similar pattern of CH_4 emissions has been found in global peatlands[44]. As such, we conclude that even if warming stimulates the decomposition of organic C in wetland ecosystems, the potential contribution of CH_4 efflux in relation to total gaseous C emissions would probably decline under future wetland drying. Even so, it should be noted that the wetland water table is also affected by locally intensive human activities[45–47]. For example, many wetlands that have been drained in the past due to land-use change are being rewetted (for example, peatland restoration in Europe), which could result in higher water tables[46,47]. As raising water levels might enhance CH_4 emissions (Supplementary Figs. 3 and 4), the coincidence of high CH_4 emission with high temperature dependence at high water table levels may further enhance the strength of climate change–CH_4 feedback. Therefore, to enhance our understanding of GHG emissions in global wetland ecosystems in a warmer world, future work is need to assess the combined effects of global climate change and human activities on wetland water tables from local to global scales.

Overall, our findings provide an empirical basis for refining representations of the temperature dependence of wetland GHG emissions in coupled climate–carbon cycle models[12,48,49]. The average temperature dependence (0.63 eV) of wetland CH_4 emissions reported here is considerably lower than that (0.96 eV) reported for anaerobic systems[18]; this discrepancy suggests that biogeochemical models may overestimate wetland CH_4 emission rates under climate warming if only the temperature dependence of CH_4 emissions under water-saturated conditions is considered. In addition, we provide evidence that the difference in the temperature dependence of wetland CO_2 and CH_4 emissions varies with WTD. The results of this study provide a cross-hydrological perspective for the analyses of the temperature dependence of wetland GHG emissions by considering both water-saturated and water-unsaturated conditions, and highlight that determining the impact of the water table on the temperature dependence of GHG emissions is critical to understanding the dynamics of wetland soil C processes in the context of global warming.

Online content

Any methods, additional references, Nature Research reporting summaries, source data, extended data, supplementary information, acknowledgements, peer review information; details of author contributions and competing interests; and statements of data and code availability are available at https://doi.org/10.1038/s41558-021-01108-4.

Received: 26 January 2021; Accepted: 30 June 2021;
Published online: 9 August 2021

References

1. Davidson, N., Fluet-Chouinard, E. & Finlayson, M. Global extent and distribution of wetlands: trends and issues. *Mar. Freshw. Res.* **69**, 620–627 (2018).
2. Mitsch, W. J. et al. Wetlands, carbon, and climate change. *Landsc. Ecol.* **28**, 583–597 (2013).
3. Lal, R. Carbon sequestration. *Philos. Trans. R. Soc. B* **363**, 815–830 (2008).
4. Nahlik, A. M. & Fennessy, M. S. Carbon storage in US wetlands. *Nat. Commun.* **7**, 13835 (2016).
5. Yvon-Durocher, G., Montoya, J. M., Woodward, G., Jones, J. I. & Trimmer, M. J. G. C. B. Warming increases the proportion of primary production emitted as methane from freshwater mesocosms. *Glob. Change Biol.* **17**, 1225–1234 (2011).
6. IPCC *Climate Change 2014: Synthesis Report* (eds Core Writing Team, Pachauri, R. K. & Meyer L. A.) (IPCC, 2014).
7. Dean, J. F. et al. Methane feedbacks to the global climate system in a warmer world. *Rev. Geophys.* **56**, 207–250 (2018).
8. Davidson, E. A. & Janssens, I. A. Temperature sensitivity of soil carbon decomposition and feedbacks to climate change. *Nature* **440**, 165–173 (2006).
9. Comer-Warner, S. A. et al. Thermal sensitivity of CO_2 and CH_4 emissions varies with streambed sediment properties. *Nat. Commun.* **9**, 2803 (2018).
10. Bridgham, S. D., Cadillo-Quiroz, H., Keller, J. K. & Zhuang, Q. L. Methane emissions from wetlands: biogeochemical, microbial, and modeling perspectives from local to global scales. *Glob. Change Biol.* **19**, 1325–1346 (2013).
11. Xu, X. et al. Reviews and syntheses: four decades of modeling methane cycling in terrestrial ecosystems. *Biogeosciences* **13**, 3735–3755 (2016).
12. Riley, W. et al. Barriers to predicting changes in global terrestrial methane fluxes: analyses using CLM4Me, a methane biogeochemistry model integrated in CESM. *Biogeosciences* **8**, 1925–1953 (2011).
13. Luo, Y. et al. Toward more realistic projections of soil carbon dynamics by Earth system models. *Glob. Biogeochem. Cycles* **30**, 40–56 (2016).
14. Chen, H., Zhu, T., Li, B., Fang, C. & Nie, M. The thermal response of soil microbial methanogenesis decreases in magnitude with changing temperature. *Nat. Commun.* **11**, 5733 (2020).
15. Kirschke, S. et al. Three decades of global methane sources and sinks. *Nat. Geosci.* **6**, 813–823 (2013).

16. Koffi, E. N., Bergamaschi, P., Alkama, R. & Cescatti, A. An observation-constrained assessment of the climate sensitivity and future trajectories of wetland methane emissions. *Sci. Adv.* **6**, eaay4444 (2020).
17. Yvon-Durocher, G. et al. Reconciling the temperature dependence of respiration across timescales and ecosystem types. *Nature* **487**, 472–476 (2012).
18. Yvon-Durocher, G. et al. Methane fluxes show consistent temperature dependence across microbial to ecosystem scales. *Nature* **507**, 488–491 (2014).
19. Segers, R. Methane production and methane consumption: a review of processes underlying wetland methane fluxes. *Biogeochemistry* **41**, 23–51 (1998).
20. Walter, B. P. & Heimann, M. A process-based, climate-sensitive model to derive methane emissions from natural wetlands: application to five wetland sites, sensitivity to model parameters, and climate. *Glob. Biogeochem. Cycles* **14**, 745–765 (2000).
21. Christensen, T. R. et al. Factors controlling large scale variations in methane emissions from wetlands. *Geophys. Res. Lett.* **30**, 1414 (2003).
22. Inglett, K. S., Inglett, P. W., Reddy, K. R. & Osborne, T. Z. Temperature sensitivity of greenhouse gas production in wetland soils of different vegetation. *Biogeochemistry* **108**, 77–90 (2012).
23. Vicca, S., Janssens, I. A., Flessa, H., Fiedler, S. & Jungkunst, H. F. Temperature dependence of greenhouse gas emissions from three hydromorphic soils at different groundwater levels. *Geobiology* **7**, 465–476 (2009).
24. Leroy, F. et al. Vegetation composition controls temperature sensitivity of CO_2 and CH_4 emissions and DOC concentration in peatlands. *Soil Biol. Biochem.* **107**, 164–167 (2017).
25. Whiting, G. J. & Chanton, J. P. Greenhouse carbon balance of wetlands: methane emission versus carbon sequestration. *Tellus B* **53**, 521–528 (2001).
26. Messager, M. L. et al. Global prevalence of non-perennial rivers and streams. *Nature* **594**, 391–397 (2021).
27. Zhu, J. et al. Modeling the potential impacts of climate change on the water table level of selected forested wetlands in the southeastern United States. *Hydrol. Earth Syst. Sci.* **21**, 6289–6305 (2017).
28. Amatya, D., Chescheir, G., Williams, T., Skaggs, R. & Tian, S. Long–term water table dynamics of forested wetlands: drivers and their effects on wetland hydrology in the Southeastern Atlantic Coastal Plain. *Wetlands* **40**, 65–79 (2020).
29. Fan, Y. & Miguez-Macho, G. A simple hydrologic framework for simulating wetlands in climate and earth system models. *Clim. Dynam.* **37**, 253–278 (2011).
30. Fan, Y., Li, H. & Miguez-Macho, G. Global patterns of groundwater table depth. *Science* **339**, 940–943 (2013).
31. Moore, T. & Roulet, N. T. Methane flux: water table relations in northern wetlands. *Geophys. Res. Lett.* **20**, 587–590 (1993).
32. Yang, J. et al. Effect of water table level on CO_2, CH_4 and N_2O emissions in a freshwater marsh of Northeast China. *Soil Biol. Biochem.* **61**, 52–60 (2013).
33. Moore, T. & Knowles, R. The influence of water table levels on methane and carbon dioxide emissions from peatland soils. *Can. J. Soil Sci.* **69**, 33–38 (1989).
34. Eyring, H. The activated complex and the absolute rate of chemical reactions. *Chem. Rev.* **17**, 65–77 (1935).
35. Lafleur, P. M., Moore, T. R., Roulet, N. T. & Frolking, S. Ecosystem respiration in a cool temperate bog depends on peat temperature but not water table. *Ecosystems* **8**, 619–629 (2005).
36. Matysek, M. et al. Impact of fertiliser, water table, and warming on celery yield and CO_2 and CH_4 emissions from fenland agricultural peat. *Sci. Total Environ.* **667**, 179–190 (2019).
37. Juszczak, R. et al. Ecosystem respiration in a heterogeneous temperate peatland and its sensitivity to peat temperature and water table depth. *Plant Soil* **366**, 505–520 (2013).
38. Yang, G. et al. Effects of soil warming, rainfall reduction and water table level on CH_4 emissions from the Zoige peatland in China. *Soil Biol. Biochem.* **78**, 83–89 (2014).
39. Zhao, M. et al. Responses of soil CO_2 and CH_4 emissions to changing water table level in a coastal wetland. *J. Clean. Prod.* **269**, 122316 (2020).
40. Olefeldt, D. et al. A decade of boreal rich fen greenhouse gas fluxes in response to natural and experimental water table variability. *Glob. Change Biol.* **23**, 2428–2440 (2017).
41. Turetsky, M. R. et al. Short-term response of methane fluxes and methanogen activity to water table and soil warming manipulations in an Alaskan peatland. *J. Geophys. Res. Biogeosci.* **113**, G00A10 (2008).
42. Cook, B. I., Smerdon, J. E., Seager, R. & Coats, S. Global warming and 21st century drying. *Clim. Dynam.* **43**, 2607–2627.
43. Xi, Y., Peng, S., Ciais, P. & Chen, Y. Future impacts of climate change on inland Ramsar wetlands. *Nat. Clim. Change* **11**, 45–51 (2021).
44. Evans et al. Overriding water table control on managed peatland greenhouse gas emissions. *Nature* **593**, 548–552 (2021).
45. Chen, H., Zou, J., Cui, J., Nie, M. & Fang, C. Wetland drying increases the temperature sensitivity of soil respiration. *Soil Biol. Biochem.* **120**, 24–27 (2018).
46. Humpenoeder, F. et al. Peatland protection and restoration are key for climate change mitigation. *Environ. Res. Lett.* **15**, 104093 (2020).
47. Manton, M. et al. Assessment and spatial planning for peatland conservation and restoration: Europe's trans-border Neman river basin as a case study. *Land* **10**, 174 (2021).
48. Gedney, N., Cox, P. & Huntingford, C. Climate feedback from wetland methane emissions. *Geophys. Res. Lett.* **31**, L20503 (2004).
49. Spahni, R. et al. Constraining global methane emissions and uptake by ecosystems. *Biogeosciences* **8**, 1643–1665 (2011).

Methods

Database compilation. Data were collected by searching for all peer-reviewed articles investigating soil CO_2 and CH_4 emissions that were published before 1 April 2020, using the Web of Science (http://apps.webofknowledge.com), the Google Scholar (https://scholar.google.com) and the China National Knowledge Infrastructure Databases (http://www.cnki.net). To avoid bias in publication selection, three criteria were used to screen the literature. (1) Both CO_2 and CH_4 emissions were measured simultaneously in the field, enabling us to calculate the response of the CH_4:CO_2 ratio to changes in the ambient temperature. (2) The studied ecosystem could be considered to represent a category of wetlands defined by the Ramsar Convention[50]: "areas of marsh, fen, peatland or water, whether natural or artificial, permanent or temporary, with water that is static or flowing, fresh, brackish or salt, including areas of marine water, the depth of which at low tide does not exceed six metres". (3) The study had a duration of at least 3 months to avoid short-term noise. Site-specific data such as latitude, longitude, mean annual temperature, water temperature, soil temperature and WTD were also obtained from the original publications, with all original data extracted from tables and figures. The software GetData (v.2.26) was used to extract the data from figures.

In total, the database comprised 3,345 paired observations of CO_2 and CH_4 emissions taken from 204 field sites across the globe (Extended Data Fig. 1). In addition, to explore whether and how the dependence of wetland GHG emissions on temperature varied with WTD, we analysed the data for the subset of sites for which simultaneous measurements of GHG emissions and WTD were available. This dataset comprised 1,580 paired observations from 88 field sites.

Statistical analyses. Mixed-effects models represent a flexible and powerful tool for performing meta-analyses of the kind of data compiled in this study. These models allow for nested covariance structures where site-level relationships are nested within overall relationships. They can also accommodate unbalanced designs in which the number of measurements varies among experimental sites. Their use enabled us to determine the overall average temperature dependence of efflux for a collection of sites while accounting for the fact that multiple efflux–temperature relationships are nested within this overall relationship; they also allowed us to explicitly quantify the variation in temperature dependence among sites.

We used linear mixed-effects modelling[51,52] to assess the temperature dependence of CO_2 and CH_4 emissions, quantified on the basis of a Boltzmann–Arrhenius function of the form:

$$\ln R_i(T) = \left(\bar{E} + \epsilon_E^i\right)\left(\frac{1}{kT_C} - \frac{1}{kT}\right) + \overline{\ln R(T_C)} + \epsilon_R^i \quad (1)$$

where $\ln R_i(T)$ represents the natural logarithm of the CO_2 or CH_4 respiration rate at absolute temperature T (K) for arbitrary site i; $\bar{E}$ is the average apparent activation energy (E) among sites, which characterizes the temperature dependence of wetland GHG emissions; and k is the Boltzmann constant (8.62×10^{-5} eV k^{-1}). We centred the temperature data using the mean temperature in the dataset, T_C, so that $\ln R(T_C)$ corresponds to the average respiration (R) rate among sites at T_C. Because biotic (for example, substrate supply, microbial community structure and/or composition, physiological acclimation and/or adaptation) and abiotic (for example, mean annual air temperature) variables may have important roles in regulating the response of GHG emissions to ambient temperature[14,18] and may vary among sites, we expected the estimates of the apparent activation energy, E, and the rate of GHG efflux at a fixed temperature, $\ln R(T_C)$, to also vary among sites. This variation was accounted for in our linear mixed-effects models by treating the slopes and intercepts as random variables with averages of $\bar{E}$ and $\overline{\ln R(T_C)}$, respectively, and defining site-specific deviations from these averages of ϵ_E^i and ϵ_R^i for each site, i. Although this statistical approach did not allow us to identify the particular variables that contribute to differences in flux–temperature relationships among sites, it did allow us to quantify the overall magnitude of their effects as standard deviations of the random-effects terms. Soil temperature at 5 cm was used to assess the temperature dependence of GHG emissions for this study. On the basis of some sites with soil temperature at different depths, it was shown that the temperature measurement depth had no significant effect on the estimated apparent activation energy (Supplementary Fig. 5). We quantified the temperature dependence of the CH_4:CO_2 emission ratio in exactly the same way as described above.

To assess whether the temperature dependence of GHG emissions was affected by the wetland water table, we divided all the GHG emission data on the basis of three WTD intervals: <−30 cm, −30 to −5 cm and >−5 cm. We then assessed the potential differences in the temperature dependence of wetland CO_2 and CH_4 emissions among these three WTD intervals. For wetlands in the '<−30 cm' WTD interval, the wetland topsoil is mainly aerobic, which is conducive to aerobic decomposition and CH_4 oxidation[35–39]. By contrast, for wetlands in the '>−5 cm' interval, the wetland soil is water-saturated, which is conducive to methanogenesis[19,40,41].

The linear mixed-effects modelling analysis was performed with the 'lme' function in the 'nlme' package in *R* statistical software (v.3.6.3)[53]. To determine whether it was necessary to include random effects corresponding to the variations in both the slope and intercept among sites[18,51,52], the likelihood ratio test was used to assess the improvement in model fit between the null model (including all potential fixed effects and only one random effect (corresponding to the intercept variation)) and an alternative model (including all potential fixed effects and both random effects (that is, those corresponding to the slope and the intercept)). By analysing the statistical results of likelihood ratio tests and comparing the Akaike information criterion (AIC) values of the two models (Supplementary Table 2), we found that the random-effects structure that best described each dataset included random variation in both the slope and intercept. Thus, we applied a random-effects structure including random variation in both the slope and intercept to assess the significance of the fixed effects (averages across sites for the apparent activation energy and intercept) and other potential covariates. We used the confidence interval overlap method[54,55] to compare the slopes and intercepts generated from the mixed-effects models corresponding to the different datasets.

The frequency distributions of relevant site-level parameters (that is, the temperature dependence of the CH_4:CO_2 emission ratio and mean WTD) were plotted to reflect their variability among the different studies on the basis of a Gaussian function (that is, a normal distribution):

$$y = ae^{\frac{(x-\mu)^2}{2\sigma^2}} \quad (2)$$

where y is the frequency of the parameter values within an interval; x is the mean of the parameter for that interval; μ and δ^2 are the mean and variance of all values of the parameter, respectively; and a is a coefficient indicating the expected value of the parameter at $x=\mu$. Origin 2021 software (OriginLab Corporation) was used to fit the data to a normal distribution.

Data availability

The original data for this study will be publicly available at: https://doi.org/10.5281/zenodo.5113602.

Code availability

The code used in this study is available from the corresponding author on reasonable request.

References

50. Matthews, G. V. T. *The Ramsar Convention on Wetlands: Its History and Development* (Ramsar Convention Bureau, 1993)
51. Pinheiro, J. & Bates, D. *Mixed-Effects Models in S and S-PLUS* (Springer Science & Business Media, 2006).
52. Zuur, A., Ieno, E. N., Walker, N., Saveliev, A. A. & Smith, G. M. *Mixed Effects Models and Extensions in Ecology with R* (Springer Science & Business Media, 2009).
53. R Core Team. *R: A Language and Environment for Statistical Computing* (R Foundation for Statistical Computing, 2020); http://www.r-project.org
54. Schenker, N. & Gentleman, J. F. On judging the significance of differences by examining the overlap between confidence intervals. *Am. Stat.* **55**, 182–186 (2001).
55. Payton, M. E., Greenstone, M. H. & Schenker, N. Overlapping confidence intervals or standard error intervals: what do they mean in terms of statistical significance? *J. Insect Sci.* **3**, 34 (2003).

Acknowledgements

We greatly appreciate the authors of the published studies who supported our data sources. We also thank J. Zou, Y. Zhang, M. Wang and other students for their contributions to the database. The National Science Foundation of China provided support for M.N. and H.C. (grant no. 91951112), B.L., M.N. and X.X. (grant no. 41630528) and C.F. and X.X. (grant no. 32030067).

Author contributions

M.N. designed the research. H.C. performed the overall analysis with the assistance from X.X., M.N., B.L. and C.F. H.C. and M.N. wrote the first draft and all authors jointly revised the manuscript.

Competing interests

The authors declare no competing interests.

Additional information

Extended data is available for this paper at https://doi.org/10.1038/s41558-021-01108-4.

Supplementary information The online version contains supplementary material available at https://doi.org/10.1038/s41558-021-01108-4.

Correspondence and requests for materials should be addressed to M.N.

Peer review information *Nature Climate Change* thanks Sophie Comer-Warner and the other, anonymous, reviewer(s) for their contribution to the peer review of this work.

Reprints and permissions information is available at www.nature.com/reprints.

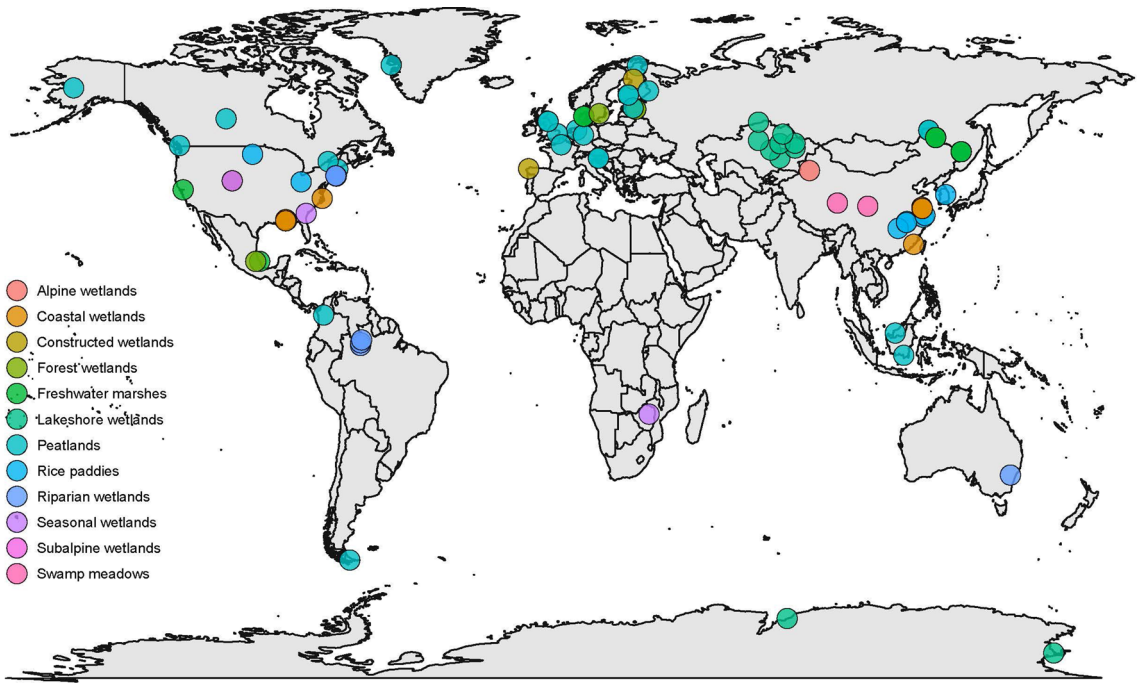

Extended Data Fig. 1 | Geographical distribution of the study sites. Some of the sites are very close to one another, and the corresponding symbols thus overlap to some extent.

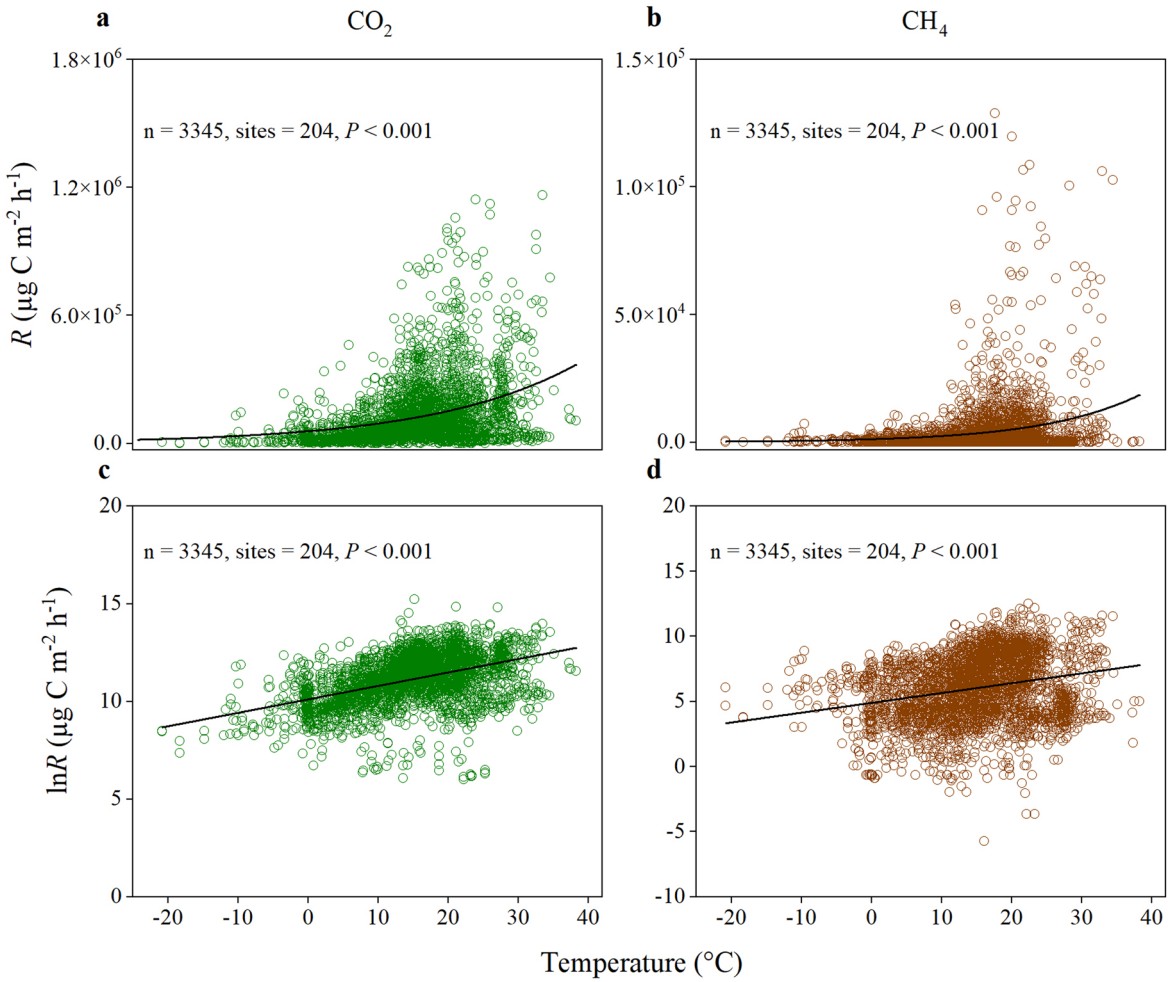

Extended Data Fig. 2 | The relationship between wetland CO_2 (a, c) and CH_4 (b, d) emission rates and temperature across 204 sites. Regression lines represent the fitted efflux–temperature exponential (**a**, **b**) and linear (**c**, **d**) relationships.

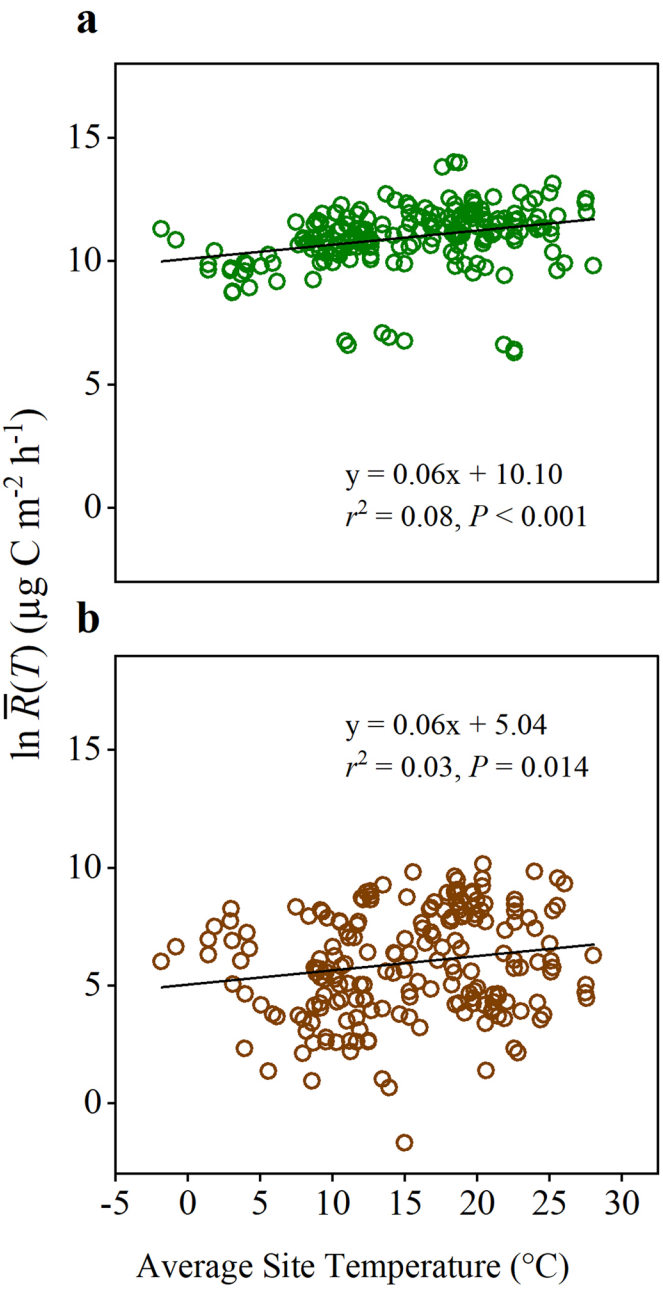

Extended Data Fig. 3 | Correlations of average site temperatures with average CO_2 and CH_4 emissions in globally distributed ecosystems. The average site temperature is positively correlated with the average CO_2 (**a**) and CH_4 (**b**) emissions, ln$\overline{R}(T)$, across 204 sites.

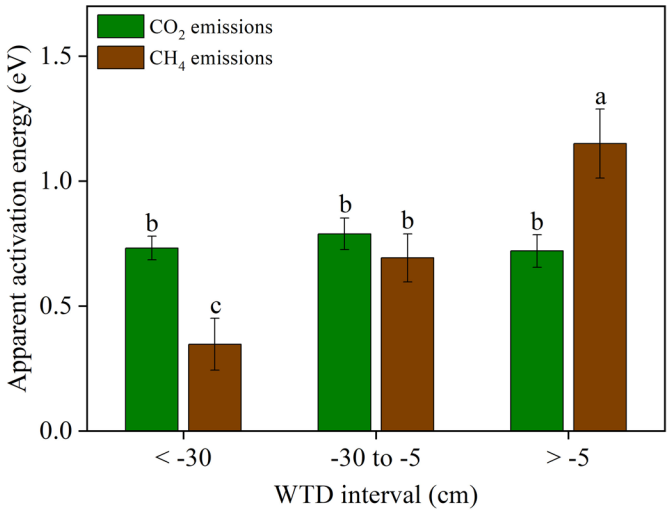

Extended Data Fig. 4 | Influence of water table depth (WTD) on the temperature dependence of wetland CH_4 and CO_2 emissions. Different letters denote significant differences ($P < 0.01$). The sample sizes by greenhouse gas type and water table depth interval are as follows: CO_2, < −30 = 332; CO_2, −30 to −5 = 675; CO_2, > −5 = 592; CH_4, < −30 = 331; CH_4, −30 to −5 = 676; CH_4, > −5 = 589. The data are represented as the mean and s.e. (the s.e. values among different water table depth intervals were obtained from the mixed-effects models).

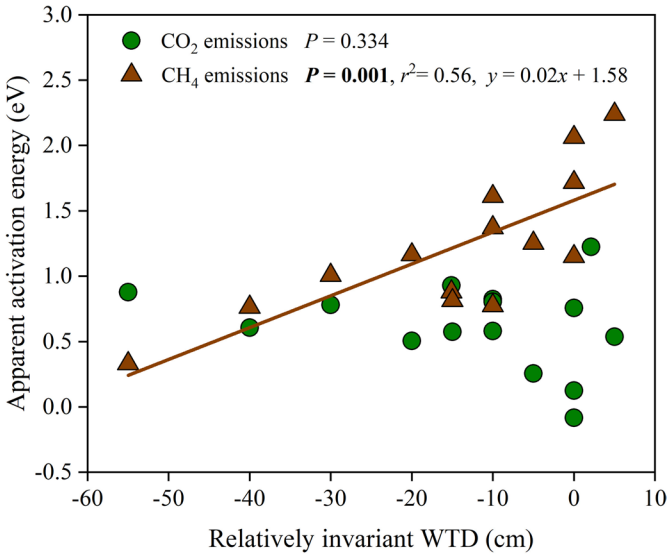

Extended Data Fig. 5 | Correlation of water table depth (WTD) with the temperature dependence of CO_2 and CH_4 emissions for wetland sites with relatively static water tables. The apparent activation energy was used to reflect the temperature dependence of CO_2 and CH_4 emissions (more details in the Method).

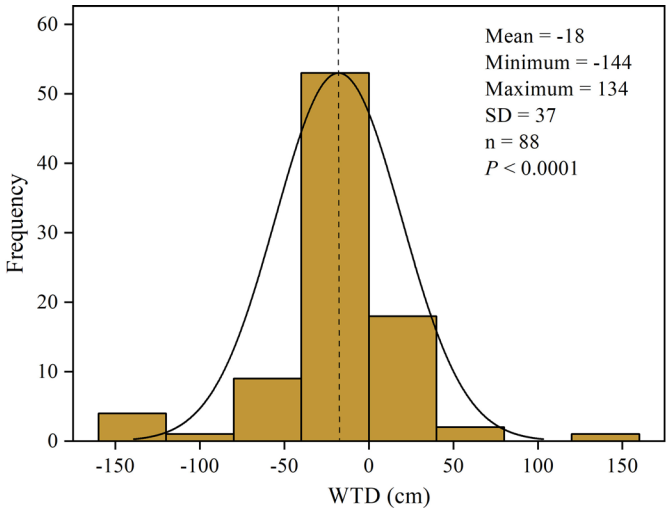

Extended Data Fig. 6 | Frequency distribution of site-level mean water table depth (WTD) values. The solid line represents a Gaussian distribution fitted to the frequency data for WTD. The distribution of site-level mean WTD values yields an average of −18 cm (represented by the dashed line).